Journal of Open Aviation Science (2023), Vol.**1**
doi:10.59490/joas.2023.7207

JOAS

PROCEEDINGS | *The 11th OpenSky Symposium*

Using ADS-B Trajectories to Measure How Rapid Exit Taxiways Affect Airport Capacity

Manuel Waltert[*,1] and Benoit Figuet[1,2]

[1]Centre for Aviation, School of Engineering, Zurich University of Applied Sciences, 8401 Winterthur, Switzerland
[2]SkAI Data Services, Zurich, Switzerland

[*]Corresponding author: manuel.waltert@zhaw.ch

(Received: 25 October 2023; Revised: 13 December 2023; Accepted: 16 January 2024; Published: 18 January 2024)
(Editor: Junzi Sun; Reviewers: Luis Delgado and Xavier Olive)

Abstract

The capacity of an airport can be specified with a so-called capacity envelope, which indicates how many take-offs and landings an aerodrome is capable of handling per unit time. In this study, the capacity envelope of an airport is determined on the basis of Automatic Dependent Surveillance-Broadcast aircraft trajectories obtained via the OpenSky Network. Trajectories are classified as departures and arrivals by using rule-based algorithms. Subsequently, the time of landing or take-off is determined for all these flight movements. Since some of the trajectories used in this study are not entirely covered near the ground, an *XGBoost* model is used to improve the determination of the take-off and landing times. In a final step, the capacity envelope is determined. To this end, the number of take-offs and landings operated at an airport within 15-minute intervals are counted first. Then, the 92.5th percentile of departures is computed for all observed arrival counts. Finally, a concave, non-increasing piecewise-linear function is fitted to these quantile values. The method introduced in this study is subsequently applied to Lisbon Airport in order to evaluate if and how the construction of an additional rapid exit taxiway has affected its capacity. The results suggest that Lisbon Airport benefits from this rapid exit taxiway. Indeed, especially when the airport handles a high number of landings, the additional rapid exit taxiway appears to allow for a slightly higher number of departures.

Keywords: Airport capacity; Capacity envelope; Rapid exit taxiways; Automatic Dependent Surveillance-Broadcast

Abbreviations: ADS-B: Automatic Dependent Surveillance-Broadcast; OSN: Opensky Network; RET: Rapid Exit Taxiway; ROT: Runway Occupancy Time

1. Introduction

The *maximum throughput capacity*, also known as the *saturation capacity*, of an airport's runway system is defined as the number of arriving and departing aircraft movements it can perform over the period of one hour, while (i) the system experiences continuous demand, and (ii) air traffic control adheres to separation requirements [1]. When being operated at maximum throughput capacity, however, airports are subject to major delays and congestion, as no level of service (LoS) requirements, such as maximum acceptable waiting times for aircraft or manageable workloads for air traffic controllers, are considered. For this reason, airports rather rely on a concept called *practical capacity* to specify the number of take-offs and landings that can be realistically achieved per unit time [2]. In practice, a number of different definitions of *practical capacity* find application. As such, the concept of *declared capacity*, where an airport declares its capacity on the basis of empirical knowledge of

experienced congestion [3], is widely used. Alternatively, the concept of *practical hourly capacity* described by the Federal Aviation Administration (FAA) is predominantly used in the United States of America [4]. Thereby, *practical capacity* is specified as the number of take-offs and landings that can be performed on a runway system under the condition that the average delay per aircraft movement is not more than four minutes.

Regardless of the definition of *practical capacity* applied at an airport, its magnitude depends on a multitude of factors. Most importantly, the number of runways available at an airport, their orientation and layout in relation to each other, dependencies between runways, as well as the *runway configuration*, which specifies how the available runways are utilised for take-offs and landings, affect capacity. This is particularly the case at airports where two or more runways are available. Moreover, for runways used for landings, the existence, location, and design of *rapid exit taxiways* (RET), which allow arriving aircraft to leave the runway at higher taxiing speeds, increase runway capacity as the average *runway occupancy time* (ROT) of landing aircraft is reduced. Besides that, an airport's capacity is affected by the actual composition of demand. In this context, both the aircraft mix, which describes the types and size of aircraft using the runway system, as well as the movement mix, which describes the percentage of take-offs and landings, are of importance. Furthermore, separation standards describing the minimum horizontal and vertical distances to be maintained between two aircraft in flight by air traffic control at all times are relevant for the determination of practical capacity. Lastly, the condition of the air traffic management system and environmental factors, such as prevailing weather conditions affect the capacity of an airport system.

To describe the capacity of an airport, two different cases must be distinguished. If a relatively short period of time is considered, for which demand, aircraft and movement mix, the applied runway configuration, weather conditions, etc., are known or given, the capacity of an airport can be expressed with two integers: the maximum number of take-offs and landings that can be performed within a certain unit of time. To estimate the capacity of an airport for such a short-run case, analytical and simulation methods, as reviewed by Newell [5] and Odoni et al. [6], can be applied. However, if airport capacity is considered over a long(er) period of time, it must be understood as a probabilistic quantity. In such a long-run case, airport capacity is often described in the literature with a concave, non-increasing envelope function φ, which specifies the dependency of the number of departing aircraft from the number of arriving aircraft as follows

$$n_{DEP} = \varphi(n_{ARR}, \theta) \tag{1}$$

where n_{DEP} is the number of departing aircraft movements per unit time, i.e., the departure count, $n_{ARR} = \{0, 1, \ldots, n_{ARR}^{max}\}$ is the arrival count, n_{ARR}^{max} is the observed maximum arrival count, and $\theta_l \in \theta$ refers to factors influencing the capacity envelope, such as weather conditions, runway configurations, etc. On the basis of observational data specifying the number of arrivals on and departures from an airport in $t = 1, ..., T$ time intervals of a given duration, the envelope function φ can be determined on an empirical basis[1]. Two different types of envelope functions are presented in the literature. Gilbo [7] presents the *capacity envelope*, which is a piecewise-linear function enveloping the *maximum* values of all observed combinations of number of departures and arrivals per time interval. Simaiakis [8] proposed the *operational throughput envelope*, which specifies the *average* number of departures and arrivals that can be handled by an aerodrome operated in a certain runway configuration per time interval.

[1] Since the envelope indicates all possible combinations of the maximum number of take-offs and landings an airport can sustain within a given time interval, the observational data used to determine the envelope should cover periods in which the airport was subject to substantial demand. Moreover, it is important to mention that the capacity envelope can only be estimated for airports which are operated (at least during some periods) at their capacity.

To increase the robustness of an envelope function φ against outliers, which can either result from errors in data collection or from the airport operating outside of its practical capacity, extreme observations should be rejected. To this end, Gilbo [7] applied a frequency-based filtering method, whereby occurrences of extreme observations which occur with a frequency below a given threshold value are excluded. Alternatively, Gilbo [7, p. 146] mentioned that rejection methods based on the "proximity of extreme observations to the nearest observations, [or] ranks of extreme values" could also be applied. Besides that, Ramanujam and Balakrishnan [9] suggested the combined usage of quantile regression and linear optimisation to robustly estimate the envelope function φ.

To determine the *capacity envelope* or the *operational throughput envelope* in practice, a rather substantial amount of data describing take-offs and landings executed at a certain airport is required. In this respect, Gilbo [7] used a made-up data set of a fictitious airport to create a *capacity envelope*. Ramanujam and Balakrishnan [9] and Simaiakis [8], however, employed data from the FAA Aviation System Performance Metrics (ASPM) database [10] and, in the case of Simaiakis [8], additional data from the Airport Surface Detection Equipment - Model X (ASDE-X)[2] to create envelopes for airports of the New York Metroplex, which includes John F. Kennedy International Airport, Newark Liberty International Airport, and New York LaGuardia Airport.

Capacity and operational throughput envelopes as well as their dependence on runway configurations and weather conditions are already well-documented in the literature. To the best knowledge of the authors, however, there are no contributions describing how the capacity envelope of an airport is affected when the runway and taxiway system of an airport is modified. Furthermore, there is no contribution in the literature in which the capacity envelope of an airport is empirically determined exclusively on the basis of Automatic Dependent Surveillance-Broadcast (ADS-B) data. In light of these gaps, this study focuses on the questions of (i) how the capacity envelope of an airport can be determined on the basis of open-source ADS-B data obtained from the Opensky Network (OSN) [11], and (ii) how the capacity envelope of an airport is affected when one or more RET are added to the taxiway system of an airport. Consequently, this study contributes to knowledge by introducing a method to generate capacity envelopes on the basis of OSN data, by evaluating and discussing the impact of RET on capacity envelopes, and by presenting an example showing how the method described in this study can be employed in practice.

The remainder of this study is structured as follows: In Section 2, a method to determine the capacity envelope of an airport on the basis of OSN-sourced ADS-B data is presented. Subsequently, Section 3 contains a practical example in which the method presented in this study is applied to a real-world example concerning the airport of Lisbon, Portugal. Finally, the results and limitations of this study are discussed in Section 4, while conclusions and outlooks are provided in Section 5.

2. Methods

In the following, it is described how a capacity envelope function for an airport can be determined on the basis of OSN-sourced ADS-B data. The remainder of this section is divided into two parts: Section 2.1 describes the methods used to create the data set employed in this study, while Section 2.2 outlines the procedure applied to determine a capacity envelope function φ for an airport on the basis of OSN trajectory data.

[2]The Airport Surface Detection Equipment - Model X (ASDE-X) is a system operated by the FAA which, at the time of writing, is in use at 35 major US airports. The system is used to track aircraft ground movements. The data required for this is obtained by fusing a number of sensors such as surveillance radars, multilateration sensors, Automatic Dependent Surveillance-Broadcast (ADS-B), Mode S, or flight plan data.

2.1 Data collection and pre-processing

To generate a data set on the basis of which a capacity envelope function φ can then be estimated for an airport, four distinctive steps were carried out. First, an airport suitable for this study had to be selected. Then, OSN data for this airport had to be obtained and pre-processed. Finally, the data quality of the take-off and landing times estimated on the basis of the OSN data had to be improved by employing machine learning methods.

Selection of airport. This study aims to measure how the addition of one or more RET to the taxiway system of an aerodrome affects its capacity envelope. Therefore, airports at which such an effect could be measured at all had to be identified first. For this purpose, it was determined which of the 100 largest airports in Europe[3] built additional RET in the period between the years 2018 and 2021[4]. Using the *historical imagery* feature provided by the *Google Earth Pro* software, the taxiway systems of the 100 largest European airports were systematically analysed for RET construction activities in the aforementioned time period. This analysis identified RET construction activities at seven airports, as summarised in Table 1.

Table 1. Shortlist of European airports which added RET to their taxiway system between the year 2018 and 2021

ICAO Code	Airport	RET identifier	Commissioning of RET(s)	Runway
EPWA	Warsaw Chopin Airport	N2	September 2020	11
EVRA	Riga International Airport	Y	July 2022	18
LEIB	Ibiza Airport	E4, E7	December 2020	06, 24
LIPZ	Venice Tessera Airport	F, G	September 2020	04R
LPPR	Porto International Airport	F1	November 2021	35
LPPT	Lisbon International Airport	H1	December 2021	20
LSZH	Zurich International Airport	B7, L7	December 2018, July 2019	28

In a further step, the quality of OSN-sourced ADS-B data in the vicinity of the airports listed in Table 1 was examined. To this end, two data sets of historical ADS-B trajectories spanning one week were downloaded for each airport via the OSN using the *traffic* library [12]: one data set for the period before RET construction and one data set for the period after RET commissioning. These two data sets were then inspected by hand for their feasibility for use in this study. In particular, it was checked whether aircraft taking-off and landing are visible, i.e., whether the coverage near the ground is given. It was found that the quality of the data varies greatly from aerodrome to aerodrome and year to year. While ground movements of most aircraft are visible for Zurich Airport, for example, the data quality in terms of ground coverage for other airports is significantly limited; trajectories of landing aircraft often end well before the threshold of the runway or only begin well after the end of the runway for departing aircraft. Furthermore, the choice of an airport suitable for this study must also take into account the influence of the COVID-19 pandemic on the traffic volume at the respective airports. To properly investigate the impact of additional RET on the capacity envelope, demand before and after the commissioning of the RET at an airport should be as unaffected as possible by COVID-related demand fluctuations on a monthly and annually aggregated level. Indeed, Zurich and Lisbon Airport are the only aerodromes listed in Table 1 that show both good[5] ADS-B

[3] A list of the 100 largest airports in Europe can be obtained from Wikipedia, for example: https://en.wikipedia.org/wiki/List_of_the_busiest_airports_in_Europe

[4] This time period was chosen to reflect the coverage and quality of OSN-sourced ADS-B data. As such, it can be assumed that both the coverage and the quality of the data are acceptable as of the year 2018.

[5] The coverage of a trajectory is considered 'good' in this study if both the air and the ground part of the trajectories are included in the data.

data quality and coverage as well as a negligible impact of COVID-19 on demand. After discussions with the local air navigation service provider *Skyguide*, however, Zurich Airport had to be excluded for further consideration in this study. According to information provided by *Skyguide*, the capacity of Zurich Airport operated in the runway configuration in which aircraft land on runway 28 is not limited by the maximum throughput of runway 28, but rather by airspace constraints. Indeed, the two RET B7 and L7 newly installed on runway 28 are used to ensure 'smooth' day-to-day operations only. Because the maximum throughput of runway 28 in Zurich does not depend on the RET but on the airspace, Lisbon Airport is used in this study as a practical example to measure the influence of RET on the capacity of a runway system.

Data collection and pre-processing. After Lisbon Airport, where RET H1 on runway 20 became operational in December 2021, was selected for further consideration, both a one-month pre-RET and a post-RET data set of ADSB-B trajectories were downloaded via OSN using the *traffic* library. To enable a comparison of the pre-RET and post-RET capacity envelopes in a later step, observation periods in which Lisbon Airport handled an equal amount of flight movements on the runway(s) of interest had to be determined. These periods were determined by downloading and systematically comparing OSN data over several months. In the end, October 2019 was selected for the pre-RET period and December 2022 for the post-RET period.

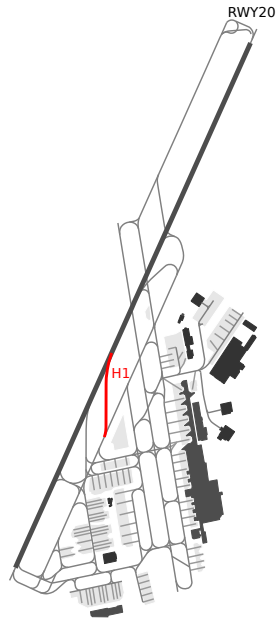

Figure 1. Airport chart of Lisbon Airport. RET H1 is indicated in red.

For both periods, data sets of OSN-sourced trajectories, which are later referred to as the pre-RET and the post-RET data set, respectively, are created as follows. In a first step, the trajectories of interest are retrieved from OSN using the *traffic* library [12]. Lisbon Airport is equipped with only one runway, namely runway 02/20, and the newly constructed RET H1, see Figure 1 and Table 1, is used by aircraft landing on runway 20. Therefore, exclusively take-offs and landings on runway 20 are further considered in this study. To identify take-offs from and landings on runway 20, rule-based algorithms are applied. As such, all trajectories that both exhibit an average climbing rate of

more than 500 feet per minute below 4,000 feet and spend at least 20 seconds in a box-shaped virtual zone located after runway 20, see Figure 2, are classified as take-offs. Similarly, all trajectories that show an average rate of climb less than 100 feet per minute and align with the extended runway axis for more than 30 seconds are assumed to be landings on runway 20. For illustrative purposes, a number of landings and departures identified in this process are depicted in Figure 2.

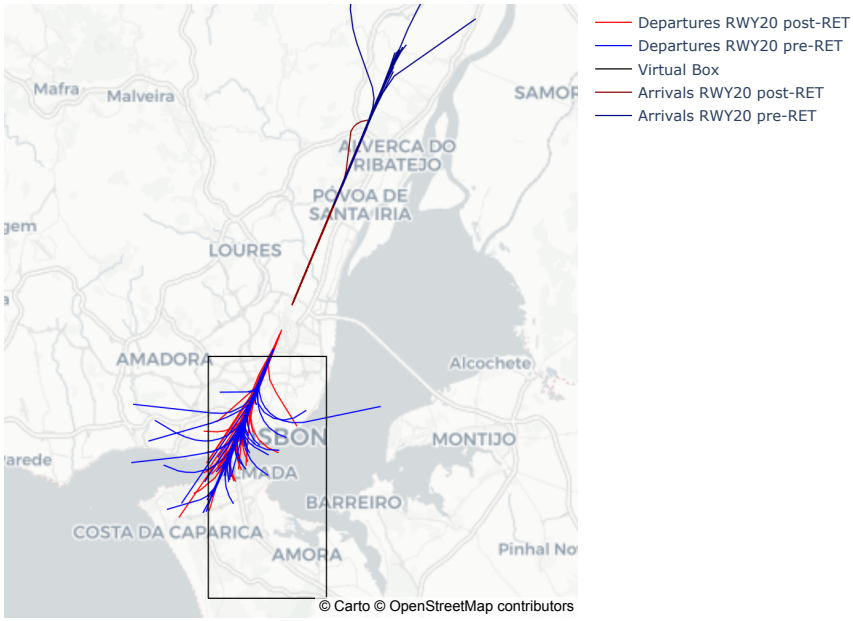

Figure 2. Sample of 200 identified departures from and 200 landings on runway 20 at Lisbon Airport. The virtual box used to identify departures on runway 20 is depicted in black.

Estimation of landing time. A visual inspection of the trajectory data revealed that the OSN-sourced trajectories of aircraft landing on airports often do not terminate on a runway, but rather some distance d_{LDG} away from its threshold. This is especially the case for trajectories of aircraft landing on runway 20 at Lisbon Airport contained in the pre-RET data set. As such, Figure 3 depicts the frequency distribution of the observed distances d_{LDG} at Lisbon Airport for the pre-RET data set and the post-RET data set with a blue and red barplot, respectively.

Since certain OSN-sourced trajectories do not end on the runway, the actual landing time of the aircraft, which is of great importance for the determination of the capacity envelope, is not known precisely enough for these flights. To improve the quality of the capacity envelope determined in this study, a machine-learning approach is applied to estimate the time aircraft require to fly distance d_{LDG}. The pre-RET and post-RET data sets are filtered in a first step for trajectories of aircraft landing on runway 20 in Lisbon that are fully covered up to the threshold. In this regard, trajectories are considered fully covered if d_{LDG} is less than 0.03 NM. In the course of this process, 544 trajectories were identified as being fully covered. From these fully covered landings, the *time to fly* to the threshold of runway 20 is computed within the last 12 NM of the approach. For this purpose, the trajectories are re-sampled at a resolution of 1 second and the distance between all resulting aircraft positions and the threshold of runway 20 is determined. Subsequently, the following six distinct features of fully covered landing trajectories are employed to predict the *time to fly*: (i) The distance of the aircraft from the threshold, (ii) the aircraft type, denoted by the ICAO aircraft type designator, (iii), the ground speed of the aircraft, (iv) the altitude of the aircraft above mean sea level, (v) the

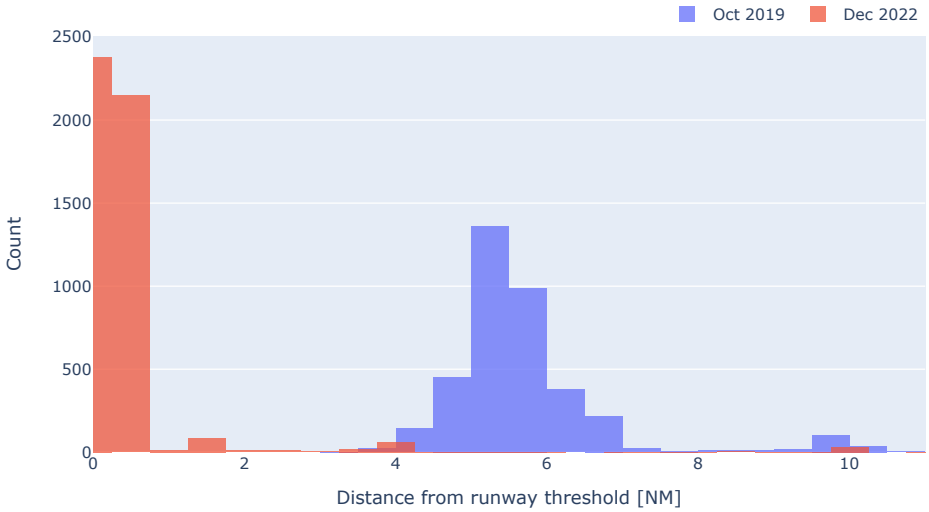

Figure 3. Observed distance d_{LDG} from the threshold of runway 20 at Lisbon Airport in NM for the pre-RET and the post-RET data sets.

aircraft track angle, and (vi) the rate of climb or descent of the aircraft. The data set of fully covered landings obtained above is split into a training, a validation, and a testing data set. While 60% of the fully covered landings are assigned on a random basis to the training data set, 20% each of the trajectories are allocated to the validation and testing sets.

Given the tabular structure of the fully covered landings data set, a gradient boosting regression approach was selected for application in this study. Specifically, the *XGBoost* library [13] is employed to build and train the model, which has a tree maximum depth of 4 and the squared error as objective function. To ensure model effectiveness and prevent over-fitting, the validation data set is utilised to halt the training process when necessary. Figure 4 illustrates the prediction obtained on the test data set. Moreover, a root mean squared error of 21.15 seconds is achieved on the tests data set.

Once the *XGBoost* model used to estimate the *time to fly* has been trained, it is applied to all trajectories of aircraft landing on runway 20 from the post-RET and pre-RET data sets. This way, the *time to fly* of every arrival flight on runway 20 and thus also their landing time is predicted.

Estimation of take-off time. Similarly to the challenges faced in estimating landing times, take-off trajectories, especially in the pre-RET data set, often lack sufficient ground coverage and become visible only a distance d_{TO} after crossing the threshold of runway 20, as shown in Figure 5. To enhance the precision of the capacity envelope estimation, a machine learning approach based on the *XGboost* model, similar to the one applied for landing time, has been developed to estimate the time required for aircraft to cover the distance d_{TO} between their initial appearance and the threshold of runway 20. Figure 6 shows the distribution of the prediction error of this model on the test data set.

2.2 Determination of envelope function

To determine the capacity envelope φ, the observation period covered by the pre-RET and post-RET data sets is divided into non-overlapping 15-minute intervals $t = 1, \ldots, T$. For each 15-minute interval t, the observed number of landings $n_{ARR,t}$ and take-offs $n_{DEP,t}$ carried out at the airport of

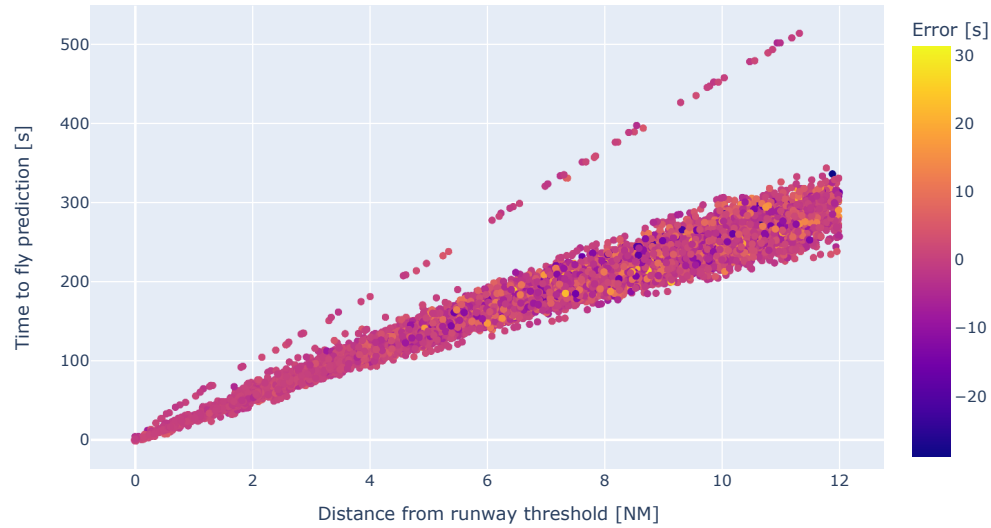

Figure 4. Prediction of remaining *time to fly* for the test data set at different distances from threshold of runway 20 at Lisbon Airport. The colour of the markers is indexed on the prediction error. Note: The data points with the considerably steeper slope of the *time to fly* prediction refer to a trajectory of a helicopter of type AgustaWestland AW139.

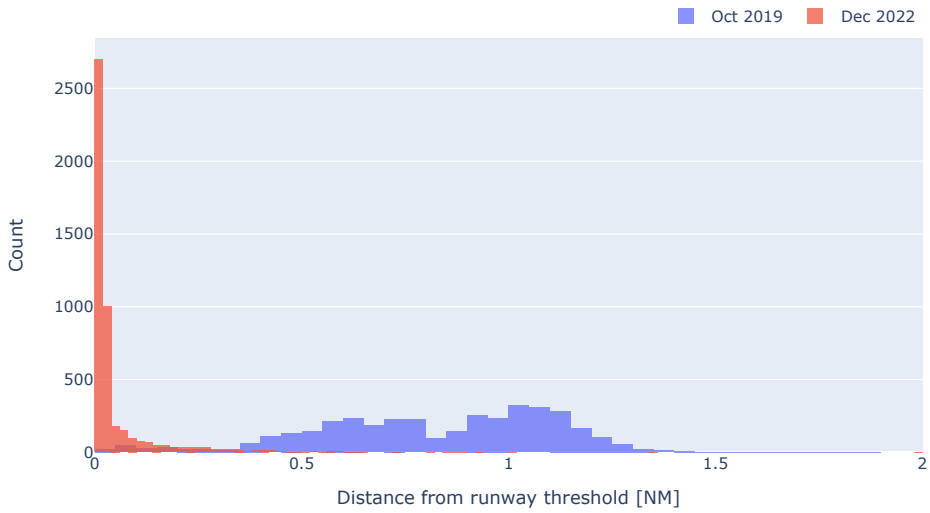

Figure 5. Observed closest distance from runway threshold in NM for pre-RET and post-RET departures.

interest is counted. This results in T tuples $(n_{ARR,t}, n_{DEP,t})$, which specify the number of observed landings and take-offs performed per interval t. The τ quantile for a given arrival count denoted $Q_\tau(n_{DEP}|n_{ARR})$ is then computed using order statistics. Subsequently, the capacity envelope φ is obtained by fitting a concave, non-increasing piecewise-linear function to the obtained quantiles as follows

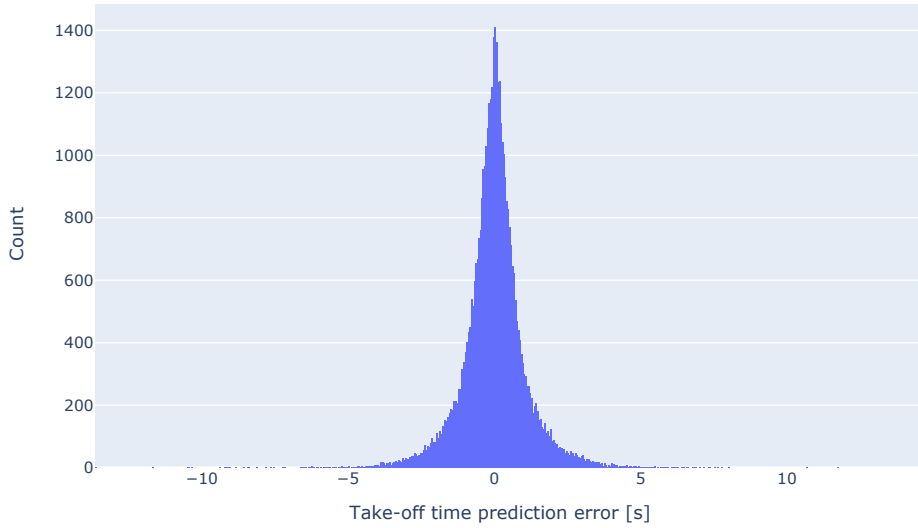

Figure 6. Error of the predicted elapsed *flight time* for distance d_{TO} of aircraft taking-off on runway 20 at Lisbon Airport for the test data set.

$$\begin{aligned} &\text{minimize} \quad \mathcal{J}(\varphi) = \sum_{n_{ARR}=0}^{n_{ARR}^{max}} \left(\varphi(n_{ARR}) - Q_\tau(n_{DEP}|n_{ARR})\right)^2 \\ &\text{subject to} \quad \varphi \in F, \end{aligned} \tag{2}$$

where F is a set of concave, non-increasing piecewise-linear functions defined on the interval $[0, n_{ARR}^{max}]$ with breakpoints at all integers between 0 and n_{ARR}^{max}. In particular, F is defined as

$$F = \left\{ f(x) = \begin{cases} L_i(x) & \text{if } i \le x < i+1 \text{ for } i = 0, 1, \ldots, n_{ARR}^{max} - 1 \\ L_{n_{ARR}^{max}-1}(x) & \text{if } x = n_{ARR}^{max}, \end{cases} \right\} \tag{3}$$

with

$$L_i(x) = m_i \cdot (x - i) + f(i). \tag{4}$$

To ensure both the non-increasing behaviour and the concavity of the capacity envelope φ, the slopes m_i of $L_i(x)$ are constrained as follows:

$$0 \ge m_0 \ge m_1 \ge \ldots \ge m_{n_{ARR}^{max}-1}. \tag{5}$$

The optimisation problem stated in Equation 2 is solved using sequential least squares programming. Moreover, as mentioned in Ramanujam and Balakrishnan [9], τ is determined in an iterative manner by selecting the highest value of τ at which the resulting capacity envelope φ experiences minimal change in response to a small variation in τ.

3. Results

This section presents the results of this study, which relate exclusively to the capacity of Lisbon Airport when aircraft arrive and depart on runway 20. Figure 7 contains two density plots summarising the relative frequency of the observed combinations of number of landings and number of take-offs $(n_{ARR,t}, n_{DEP,t})$ per 15-minute interval t. The density plot on the left refers to the pre-RET data set, the plot on the right to the post-RET data set. Combinations of $(n_{ARR,t}, n_{DEP,t})$ that occur frequently are highlighted in dark red, less frequent combinations are coloured light red, unobserved combinations ar

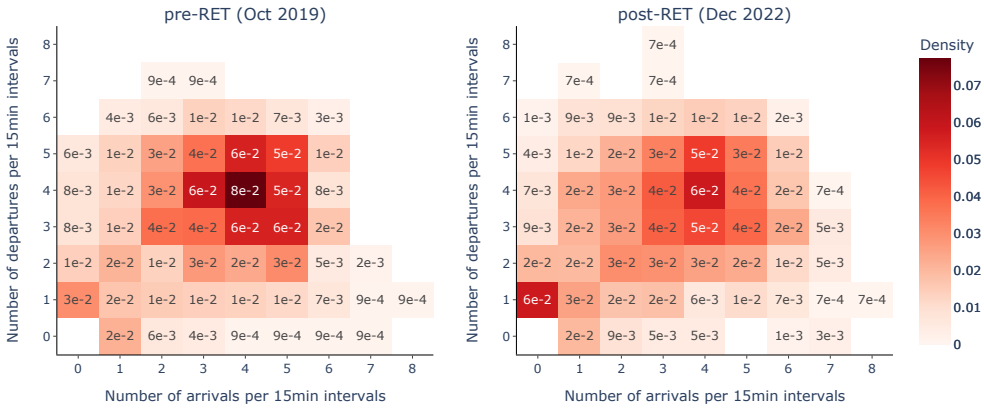

Figure 7. Observed density for number of arrivals and departures per 15-minute intervals.

Figure 8 contains the capacity envelope φ as well as the $Q_\tau(n_{DEP}|n_{ARR})$ values of Lisbon Airport for both the pre-RET and the post-RET data sets. Features referring to the pre-RET data set are drawn in blue, while post-RET features are coloured in red. The capacity envelopes, which become stable at $\tau = 0.925$, are illustrated with line plots. Moreover, The 92.5th percentile values $Q_\tau(n_{DEP}|n_{ARR})$ for all observed values of $n_{ARR} = 0, 1, \ldots, n_{ARR}^{max}$ are shown as scatter points.

4. Discussion

The density plots in Figure 7, which illustrate the relative frequency of the value combinations of the observed number of take-offs and number of landings per 15-minute interval $(n_{ARR,t}, n_{DEP,t})$, suggest that the density is better distributed within the envelope in the post-RET case than in the pre-RET data set. In particular, it is noticeable that the magnitude of the maximum density value in the post-RET data set is lower than in the pre-RET data set. Besides, the figure further reveals that, when frequented by a *high* number of landings (i.e., $n_{ARR} = 7$), Lisbon Airport tends to be capable of operating more departures in the post-RET than the pre-RET case. While the impact of the shift of the density distribution on the operation of the airport is difficult to interpret, the increase in departure output at high landing volumes might be a first indication of an increase in capacity potentially enabled by the additional RET.

A (slight) increase in the capacity of Lisbon Airport in the post-RET case can also be concluded from the data shown in Figure 8 for a number of reasons. First, the 92.5th percentile values, i.e., the scatter points, are post-RET on average higher than pre-RET. Here it is particularly noticeable that for $0 \leq n_{ARR} \leq 5$ the 92.5th percentile values are more dispersed in the post-RET than the pre-RET case. This increase in variance might suggest that the *true* capacity of the airport could not be entirely captured

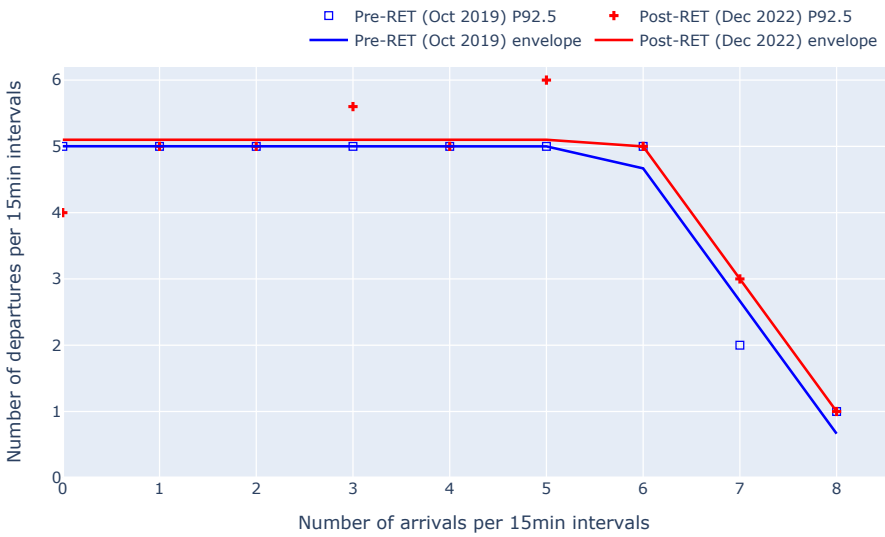

Figure 8. Observed capacity envelopes and 92.5th percentile values $Q_\tau(n_{DEP}|n_{ARR})$ of Lisbon Airport for the pre-RET (blue) and the post-RET (red) data sets.

in the post-RET data set used in this study, as the airport has most probably never been operated at its capacity during the selected observation period. This circumstance confirms the literature [1, 7, 9], according to which the actual measurement of airport capacity poses a difficult undertaking. For exactly this reason, Simaiakis [8] measures the capacity of an aerodrome in situations when congestion and delays are visible, e.g., when queues of departing aircraft are formed at the holding points of the runways. However, as will be discussed later, such an approach is not implementable in this study due to limited ground coverage of OSN data. Another indication of increased capacity in the post-RET case can be inferred from the capacity envelopes shown in Figure 8. As such, the post-RET capacity envelope encloses the pre-RET envelope over the entire observed spectrum of n_{ARR} values. For $n_{ARR} \leq 5$ it is noticeable that the two envelopes hardly differ from each other, while for $n_{ARR} > 5$ more pronounced dissimilarities are visible. This behaviour was to be expected because RET exclusively influence the ROT of landing aircraft: Only when a sufficient number of arrivals $n_{ARR,t}$ are handled per time 15-minute interval t, the capacity increase provided by a RET becomes apparent. At $n_{ARR} \leq 5$, Lisbon Airport can handle approximately five departures per 15 minutes before and after the installation of the additional RET. Under these conditions, 40 aircraft movements can be realised per hour, which relates to an average ROT of 90 seconds per aircraft movement. However, if seven landings are performed per 15-minute interval, for example, the airport's 92.5th percentile value $Q_\tau(n_{DEP}|n_{ARR})$ is equal to two departures under pre-RET conditions and three departures in the post-RET case. Consequently, at high arrival loads, the installation of the RET appears to allow the hourly number of movements to be increased from 36 to 40 and the average ROT to be decreased from 100 to 90 seconds per aircraft movement.

This study is subject to limitations. In addition to the already mentioned fact that capacity envelopes are difficult to measure empirically, high demands are placed on the input data used to determine envelopes. This is particularly the case if the time of a take-off or landing is to be inferred on the basis of trajectory data. In theory, if a trajectory contains both the air and ground portions of a flight, the take-off or the landing times can be determined rather straightforward. For most European airports, however, it has been found that (i) the ground part of OSN-sources trajectories is missing, and (ii) the

airborne part of trajectories is often not well covered near ground. The reason for this lack of data lies in both the spatial and temporal coverage of OSN. In terms of spatial coverage, it is noticeable that the ground coverage of OSN is limited at most European airports. Had the coverage been better, important information on the ROT of aircraft as well as on how the RET are used in day-to-day operations could have been collected. However, improving ground coverage is a difficult endeavour, as additional ADS-B receivers would have to be placed in the immediate vicinity of aerodromes that are still poorly covered today. With regard to temporal coverage, substantial improvements have been realised by the OSN for most regions in Europe in recent years[6]. This circumstance is also reflected in a visible reduction of the average distances d_{LDG} and d_{TO} between the pre-RET and the post-RET data sets, see Figures 3 and 5. Indeed, it was only thanks to the significantly better data quality in the post-RET data set that an *XGBoost*-based machine-learning approach could be used in this study to estimate the take-off and landing times of the poorly covered trajectories. This way, the significance and validity of this study has been improved considerably.

Besides data coverage-related issues, the results of this study are also affected by the effects of the COVID-19 pandemic on air traffic demand. In order to enable a fair comparison of airport capacity before and after the installation of a RET, only airports for which the pre-RET and post-RET data sets contain approximately the same number of aircraft movements on an aggregated level (e.g. per month) were considered. As many airports in Europe have not yet fully recovered from the effects of the pandemic by the year 2023, the number of candidate airports to consider is severely limited. Finally, it must be mentioned that only one factor θ_l influencing the capacity envelope, namely the existence of an additional RET, was considered. If additional factors θ_l, such as weather conditions or runway configurations, were taken into account, statements even more relevant for the operation of an airport could be made. However, this would require the pre-RET and post-RET data sets to cover more than one single month.

5. Conclusion and Outlook

This study introduced a method to measure the capacity envelope of airports based on OSN-sourced aircraft trajectory data. For this purpose, trajectories tracked in the vicinity of an airport were downloaded via OSN for an observation period of one month. The flights taking off and landing at this airport were identified using rule-based algorithms. Because the coverage of trajectories near the airport is sometimes limited, the data quality has been improved with a *XGBoost* model. Finally, the capacity envelope of the airport was determined by counting the number of departures and arrivals the aerodrome handled per 15-minute intervals over the entire observation period, calculating the τ quantile of departures for any observed number of landings per 15-minute interval, and fitting a concave, non-increasing piecewise-linear function to the τ quantile values.

The method presented in this study was applied to the example of Lisbon Airport in order to demonstrate how the construction of an additional RET affected the aerodrome's capacity. The results suggest that, as supported by the literature, additional RET positively influence the capacity envelope of Lisbon Airport: In particular, if the airport performs (relatively) many landings per 15-minute interval, the number of departures can be increased as the additional RET appears to reduce the average ROT of the landing aircraft slightly.

By determining the capacity envelope of an airport, this study demonstrated exemplary that OSN-sourced trajectory data can be effectively employed to analyse and evaluate the day-to-day operations of airports and airlines. For this reason, several extensions to this research are possible. Most obviously, the expansion of the observation period of both the pre-RET and post-RET data sets would

[6]Based on the authors' personal experience with OSN data, the coverage for most airports and regions in Europe is acceptable as of the year 2018.

enable the investigation of the influence of other factors θ_l such as the weather on the capacity envelope. Furthermore, the influence of other infrastructure elements on the capacity envelope, such as adjustments to holding points (e.g., number and/or arrangement) or maintenance of runways could be analysed. In addition, it must be mentioned at this point that, if the quality and coverage of trajectory data near-ground and on-ground were even better, a completely new field of research would open up. In this case, one could investigate the taxiing characteristics of aircraft on the ground, the turn-around performance of airlines, or the scheduling of flights at congested airports.

Acknowledgement

The authors acknowledge the contributions of three anonymous reviewers that greatly enhanced the value of this study. No potential conflict of interest was reported by the authors.

Author contributions

- Manuel Waltert: Conceptualization, Methodology, Writing–Original draft, Project administration
- Benoit Figuet: Conceptualization, Data curation, Methodology, Software, Writing–Review & Editing

Open data statement

The software code used to download the OSN data employed in this study is available on the following repository: https://github.com/figuetbe/OSN23-RET

Reproducibility statement

The software code used to train the applied *XGboost* model, and to generate the results presented is available on the following repository: https://github.com/figuetbe/OSN23-RET

References

[1] Richard De Neufville, Amedeo R Odoni, Peter P Belobaba, and Tom G Reynolds. *Airport systems: Planning, design, and management*. McGraw-Hill Education, 2013.

[2] National Acedemies of Science, Engineering, and Medicine. *Evaluating airfield capacity*. Washington, DC: The National Academies Press, 2012. DOI: 10.17226/22674.

[3] Airport Council International. *Airport capacity: Guidance on airport capacity declarations*. Montréal, Canada, 2023.

[4] Federal Aviation Administration. *Airfield and airspace capacity delay analysis*. Report FAA-APO-81-14. Office of Aviation Policy and Plans, Washington, DC, 1981.

[5] Gordon F Newell. "Airport capacity and delays". In: *Transportation Science* 13.3 (1979), pp. 201–241. DOI: 10.1287/trsc.13.3.201.

[6] Amedeo R Odoni, Jeremy Bowman, Daniel Delahaye, John J Deyst, Eric Feron, R John Hansman, Kashif Khan, James K Kuchar, Nicolas Pujet, and Robert W Simpson. *Existing and required modeling capabilities for evaluating ATM systems and concepts*. Tech. rep. 2015.

[7] Eugene P Gilbo. "Airport capacity: Representation, estimation, optimization". In: *IEEE Transactions on Control Systems Technology* 1.3 (1993), pp. 144–154.

[8] Ioannis Simaiakis. "Analysis, modeling and control of the airport departure process". PhD thesis. Massachusetts Institute of Technology, 2013.

[9] Varun Ramanujam and Hamsa Balakrishnan. "Estimation of arrival-departure capacity tradeoffs in multi-airport systems". In: *Proceedings of the 48h IEEE Conference on Decision and Control (CDC) held jointly with 2009 28th Chinese Control Conference*. IEEE. 2009, pp. 2534–2540.

[10] Federal Aviation Administration. *FAA Operations & Performance Data*. URL: https://aspm.faa.gov/ (visited on 09/22/2023).

[11] Matthias Schäfer, Martin Strohmeier, Vincent Lenders, Ivan Martinovic, and Matthias Wilhelm. "Bringing up OpenSky: A large-scale ADS-B sensor network for research". In: *IPSN-14 Proceedings of the 13th International Symposium on Information Processing in Sensor Networks*. IEEE. 2014, pp. 83–94.

[12] Xavier Olive. "traffic, a toolbox for processing and analysing air traffic data". In: *Journal of Open Source Software* 4.39 (2019), pp. 1518–1. DOI: 10.21105/joss.01518.

[13] Tianqi Chen and Carlos Guestrin. "XGBoost: A scalable tree boosting system". In: *Proceedings of the 22nd ACM SIGKDD International Conference on Knowledge Discovery and Data Mining*. San Francisco, California, USA, 2016, pp. 785–794. DOI: 10.1145/2939672.2939785.